HOP-DERIVED XANTHOHUMOL INDUCES HL-60 LEUKEMIA CELLS DEATH

Brown H[1], Rieland A[2], Pacurari M[1*]

[1]Department of Biology, College of Science, Engineering and Technology, Jackson State University, Jacksons MS, 39217, USA

[2]School of Medicine, Howard University, Washington DC, USA

* *Corresponding author:*

Maricica Pacurari, PhD; Department of Biology, College of Science, Engineering and Technology, Jackson State University, Jacksons MS, 39217, USA
Email: maricica.pacurari@jsums.edu

Abstract

Background. Acute promyelocytic leukemia (APL) affects both kids and adults, however it is more prevalent in younger population. Although APL has a favorable prognostic, patients that relapse often do not respond positively to additional chemotherapy. Therefore, there is a need to further identify ways to overcome these challenges.

Hypothesis: In this study, we examined antileukemic effects of xanthohumol (XN), a prenylated flavonoid derived from hops (*Humulus lupulus L*), on human promyelocytic HL-60 cells.

Materials and Methods. HL-60 cells were exposed to different concentrations of XN (μM) for 24 h. Cell viability, cell morphology, chromatin condensation, cPARP-1 level, and caspase-3 activation, and the expression of $p21^{WAF1/Cip1}$ were analyzed.

Results. XN reduced HL-60 cell viability in a dose-dependent manner. XN induced a dose-dependent morphological changes including cell shrinkage and blebbing, and significantly increased the number of cells with condensed chromatin. XN significantly increased the level of cPARP-1, active caspase-3, and the expression of $^{p21WAF/CIP}$ mRNA.

Conclusion. These data indicate that XN induces HL-60 cell death by regulating cell cycle progression and apoptosis. This study suggests that XN may have antileukemic preventive effects.

Key words: Acute promyelocytic leukemia, apoptosis, caspase-3, p21, xanthohumol, plant derived, HL-60 cells

Abbreviations

APL acute promyelocytic leukemia

PARP-1 polymerase associated reactive protein 1

cPARP-1 cleaved PARP-1

FBS Fetal Bovine Serum

XN xanthohumol

Introduction

Acute promyelocytic leukemia (APL) is a subtype of acute myeloid leukemia (AML) and represents approximately 5-20% of AML cases. Each year about 600-800 new cases of leukemia are diagnosed in the USA [1]. Although APL has a good prognosis however if the diseases is untreated or relapses, the mortality rate is high and approximately 30% of patients relapse [2-3]. Epidemiologic studies show that APL is more common in children and young adult patients and among Hispanics [4]. Although new therapeutic approaches have been developed, APL still remains an aggressive subtype of AML and with high rates of early death [5-6]. Indeed, approximately 17.3% of cases undergo early death within one month of diagnosis due to severe hemorrhages [7]. Therefore, finding new approaches to improve APL treatment outcome is of great importance. Plant-based compounds alone or in combination with chemodrugs have been shown to have antitumor effects and to improve treatment outcome of several malignant hematologies including Hodgkin's disease and acute lymphoblastic leukemia [8-11]. For example, plant-derived alkaloids vincristine and vinblastine are approved for the treatment of hematological malignancies and other cancers [10-11]. Vincristine is used to treat childhood leukemia whereas vinblastine is used in combination with chemodrugs to treat breast and bladder cancers [12-14]. Although vincristine is successful for childhood leukemia often leads to neuropathy 14-15]. Thus identifying plant compounds with antileukemic properties and less toxicity will contribute to improve treatment outcome [11, 16-17]). Plant-derived prenylated flavonoid, xanthohumol (XN), has been shown to have biological properties. XN is present in the cones of hop plant (*Humulus lupulus L*) Fig. 1 [18].

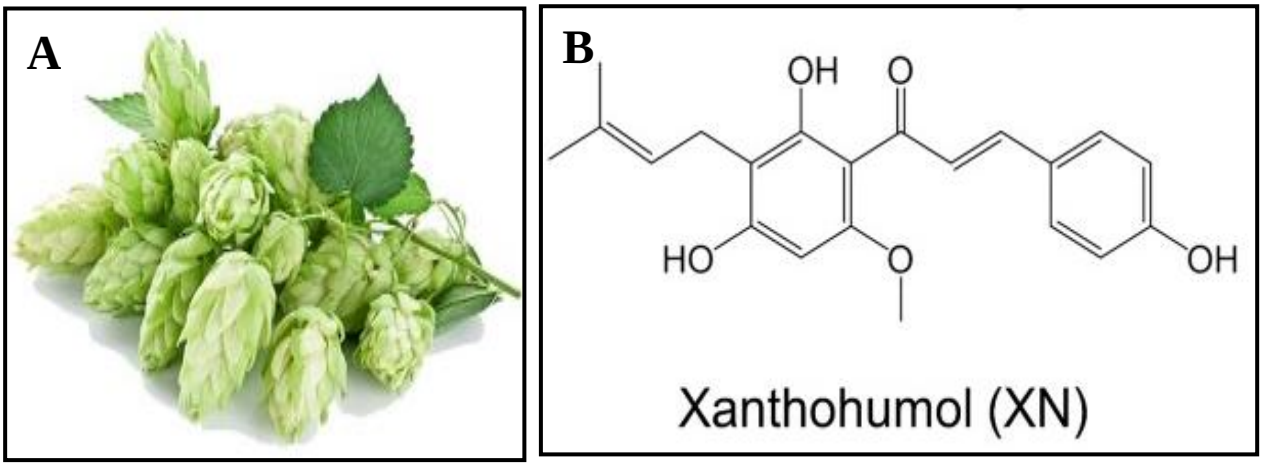

Figure 1. Hop plant cones (*Humulus lupulus L*) (**A**), and XN chemical structure (**B**). XN is a prenylated chalcone found in the cones of hop plant [18].

In hops, XN content vary from 0.1% to 1% dry weight [19]. In addition of being used in brewing industry, numerous studies also showed XN's numerous biological effects including anti-inflammatory, anti-oxidant, and anti-infectious [20-23]. Recent studies showed XN increased lipid and glucose metabolism [24-26]. Anti-carcinogenic properties have been shown on many different cancer cell types including liver, prostate, endometrial, colon, and lung [26-31]. The exact mechanism by which XN exerts its effects is not fully understood, however studies suggest that it inhibits cell proliferation and induces apoptosis by upregulating p53, inducing S phase cell cycle control genes, and downregulation of hexokinase II-mediated glycolysis [31-32].

While anti-carcinogenic effects were studied on many cancer cell types, fewer studies examined XN's effects on human acute promyelocytic leukemia. In the present study, we examined the effects of XN on acute promyelocytic leukemia HL-60 cells.

Materials and Methods

Chemicals. XN was purchased from Sigma Aldrich (Saint Louis, MO). Caspase-3 assay kit was purchased from Thermofisher Scientific/Invitrogen (Waltham, MA), MTT assays was purchased from Promega (Madison, WI), and Hoechst 33258 was purchased form Thermofisher Scientific/Molecular Probes, whereas PARP-1 antibody was purchased from Cell Signaling Technologies (Danvers, MS).

XN preparation. XN was prepared in DMSO according to the methods previously described [27]. A stock solution (50 mM) was prepared and kept at -20°C and used within 2-3 weeks. For cell culture studies, the stock solution was further diluted to various concentrations in the basal media before cell treatment thus achieving a final concentration of 0.1% DMSO.

Cell culture. Human acute promyelocytic leukemia HL-60 cell line was purchased from the American Type Culture Collection (ATCC, Manassas, VA). HL-60 cells were cultured in Iscove's Modified Dulbecco's Medium (IMDM) supplemented with penicillin, streptomycin, L-glutamine and 20% fetal bovine serum. The cells were cultured at 37˚C in humidified incubator with 95% air and 5% CO2.

Cell viability. Cell viability was measured using Celltiter 96 Aqueous One Solution Cell Proliferation Assay according to the protocol provided by the manufacturer (Promega Inc, Madison, USA). Briefly, this assay contains tetrazolium compound (3-(4,5-dimethylthiazol-2-yl)-5-(3-carboxymethoxyphenul)-2-(4-sulfophenyl)-2H-tetrazolium salts; MTS) and an electron coupling reagent (phenazine ethosulfate; PES). The MTS tetrazolium compound is reduced by cells into a colored formazan product that is soluble. The cells were subcultured in 96-well plates

at a density of 10,000 cell/well in 5% FBS/DMEM/Penicillin/Streptomycin (10,000/1000 units) for 24 h at 37ºC/5% CO_2. After 24 h, the cells were treated with XN at 6.25, 12.5, 25, and 50 µM for 24 h. After 24 h of treatment, 20 µl of tetrazolium were added to the cells and incubated for 4 h at 37ºC/5%CO_2. After 4 h, 25 µl of 10% SDS were added and the plate was incubated for 18 h at room temperature in a humidified container. After 18 h, the absorbance was measure at 490 nm using a 96-well microplate reader (SpectraMax 190, Molecular Scientifics, NH).

RNA isolation. Total RNA was extracted using Trizol® (Invitrogen, CA) according to the manufacturer's protocol. To ensure a good RNA quality, the integrity and quality of the total RNA was evaluated using 28S/18S ratio and a visual image of the 28S and 18S bands were evaluated on the 2100 Bioanalyzer (Agilent Technologies, Santa Clara, CA). Concentration of the total RNA was assessed using the NanoDrop-1000 Spectrophotometer (NanoDrop Technologies, Germany).

Quantitative real-time (q)PCR. qPCR for target genes was determined using total RNA and cDNA was generated using a High-Capacity cDNA Reverse Transcription kit and TaqMan gene expression assays (Applied Biosystems Inc., CA). The levels of p21 and 18S mRNA was measured using SYBR-Green Master mix and gene specific primers according to manufacturer's protocol (Applied Biosystems Inc.). All qRT-PCR reactions were performed on 7500 instrument (Applied Biosystems Inc.). In the qRT-PCR analysis of genes, the dissociation curve showed the absence of a secondary peak, indicating no presence of primer dimer. The expression level of each gene was determined by following formulas: fold change = $2^{-\Delta\Delta Ct}$, where ΔCt (cycle threshold) = $Ct_{\text{target gene}} - Ct_{\text{endogenous control gene}}$, and $\Delta\Delta Ct = \Delta Ct_{\text{treated sample}} - \Delta Ct_{\text{control sample}}$. 18S was used as an endogenous control gene [33-34].

Western blot. After treatments, the cells were lysed in 1X SDS lysis buffer (50 mM Tris-HCl, pH 6.8, 2% SDS, 10% glycerol). Total protein was quantified by the BCA method. β-mercaptoethanol was added to lysates to a final concentration 100 mM. Equal amounts of total protein were separated by 4-12% SDS-PAGE and transferred to a PVDF membrane. Membranes were blocked with 5% non-fat milk in 1X PBS containing 0.05% Tween-20 for 1 h at room temperature. Membranes were then incubated with PARP-1 primary antibody (Cell Signaling Technologies) at 4ºC overnight. After the incubation the membranes were washed three times in 1X PBS with 0.05% Tween-20 for 10 min and then incubated for 1 h at room temperature with horseradish peroxidase (HRP) conjugated goat anti-mouse IgG in 5% non-fat milk/1X PBS/ 0.05% Tween-20. Membranes were then washed five times for 10 min in 1X PBS with 0.05% Tween-20 and the proteins were visualized using an ECL Chemiluminescence Kit (Millipore, MA). Relative protein level was determined after normalization to beta-actin.

Cell morphology. The cells were cultured in 6-well plates in 5%FBS/IMDM/Penicillin/Streptomycin for 24 h at 37ºC/5% CO_2. After 24 h, the cells will be treated with 6.25, 12.5, and 25 µM of XN in basal media for 24 h. After 24 h, the cell morphology micrographs were taken using phase-contrast inverted microscopy. Images will be captured using a Carl Zeiss Axiovert 200 microscope equipped with Spot Camera.

Nuclear staining with Hoechst 33258. The cells were seeded on cover slips in 6-well plates and allowed to grow overnight. The cells were treated with various concentrations of XN for 24 h. At the end of the incubation period, the cells fixed in 10% paraformaldehyde/PBS for 20 min at RT, and the plate spun down at 1000 rmp for 2 min, and washed with cold PBS. The cells were stained with fluorescent dye Hoechst 33258 (10 µg/ml; Molecular Proves, NY) and incubated for 15 min at RT. The slides were examined and the apoptotic cells were identified according to the

condensation and fragmentation of their nuclei observed under Olympus IX70 microscope (Olympus Optical Co., Ltd, Japan) equipped with a Retiga 2000R FAST camera (Qimaging, Canada). Images were acquired using SimplePCI software (Compix Inc., Sewickley, PA).

Human Caspase-3 (active) ELISA assay. The cells were cultured in growth media and after 24 h the media was changed to basal media and XN was applied for 24 h. After the treatment, the cells were washed, scraped off in 1 X PBS and spun down at 5,000 rpm for 3 min and the pellet was lysed in cell RIPA extraction buffer (Thermofisher Scientific) with 1 mM PMSF, and protease inhibitor (Sigma Aldrich) on ice and sonicated 10 sec on ice, and then centrifuged at 14,000 rpm for 10 min at 4ºC. The samples were further diluted 10X in assay's standards' diluent buffer. Caspase-3 assay was performed according to manufacturer's protocol (Thermofisher Scientific/Invitrogen).

Statistical analysis. Data are presented as mean ± SEM from three experiments. Statistical analysis was performed using one-way analysis of variance (ANOVA) and Student's paired *t*-test with a significance level of $p \leq 0.05$ versus non-treated control samples.

Results

XN effect on cell viability

The effect of XN on the proliferation of HL-60 cells was determined using MTT assay. The HL-60 cells were treated with 6.25, 12.5, 25, or 50 µM of XN for 24 h (Figure 2). XN significantly decreased HL-60 cells viability at 12.5, 25, and 50 µM compared to control ($p < 0.05$, Figure 2).

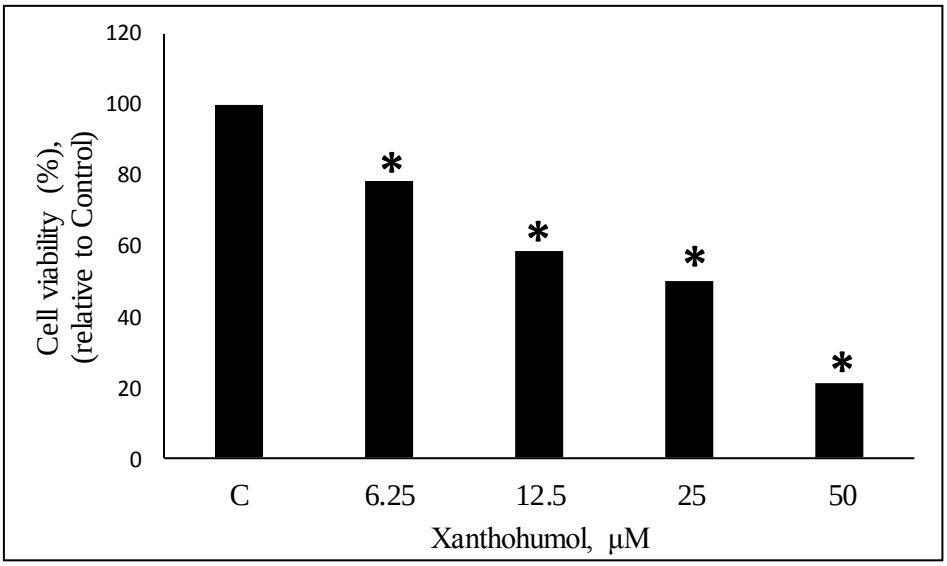

Figure 2. The effect of XN on the viability of HL-60 cells. The cells were treated with 6.25, 12.5, 25, and 50 μM of XN for 24 h. After 24 h of treatment cell viability was measured using Cell Titer 96 Aqueous One Solution Assay as described in Materials and Methods. Data is presented as % cell viability relative to control, n = 3, * Statistically significant, ANOVA, $p < 0.05$ vs control.

XN effect on cell morphology

The effect of different concentrations of XN on cell morphology were analyzed using light microscopy. At 6.25 μM, XN did not induce profound cell morphology changes compared to control cells, although some cells displayed vesicles and mild shrinkage (Figure 3, arrow). At concentrations higher than 6.25 μM, XN induced strong cell morphological changes such as cell-size shrinking and rounding, and formation of cytoplasmic visible vesicles (Figure 3, dashed arrow). At the highest tested concentration of 25 μM, XN induced profound cell rounding, shrinking, and a reduction in cell number (Figure 3, arrow and dashed arrow).

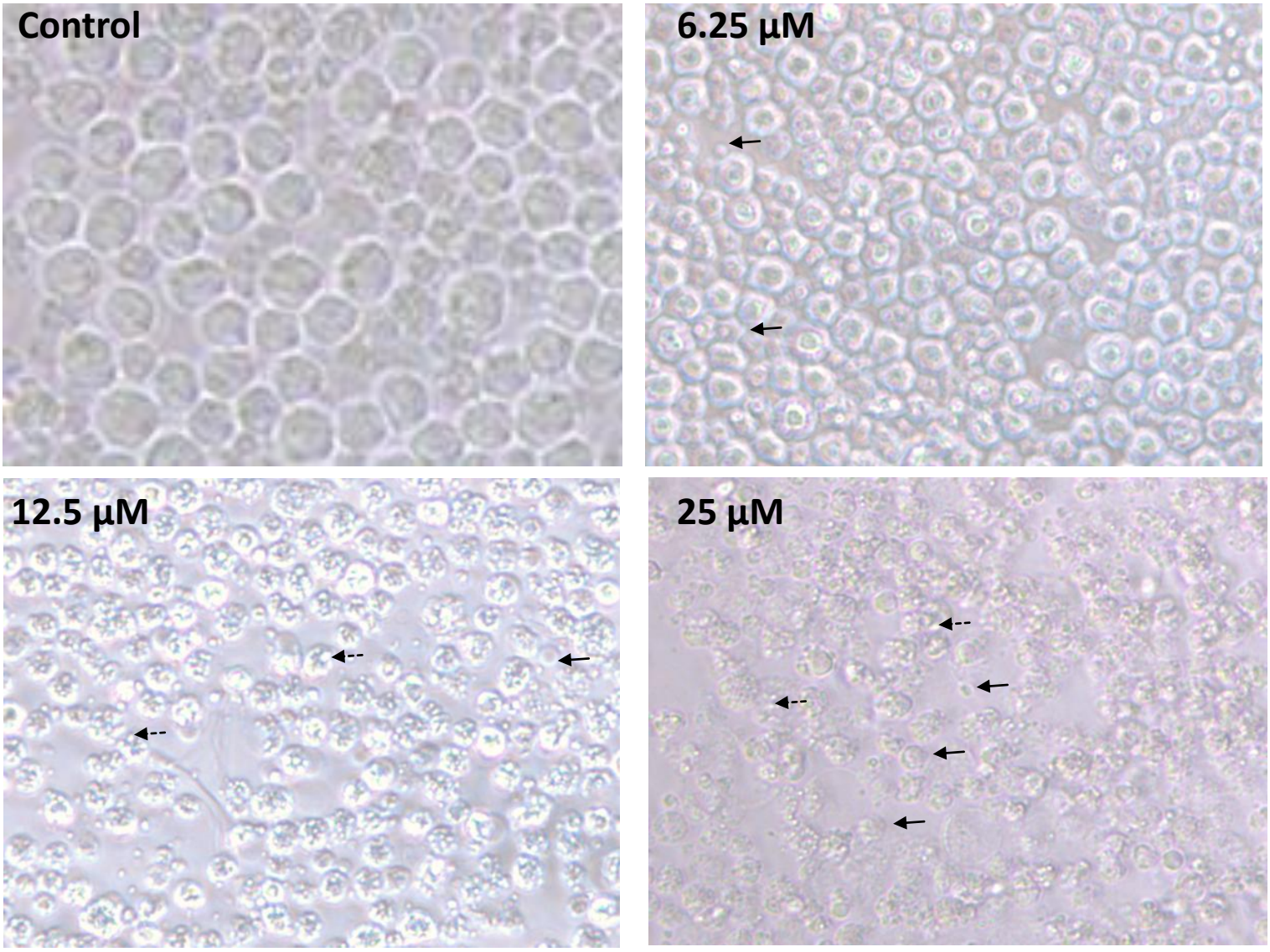

Figure 3. Cell morphology changes in the absence and presence of XN. HL-60 cells were grown in 5% FBS growth media for 24 h followed by treatment with different concentrations of XN (µM) as shown in the figure for 24 h. Representative micrographs of one experiment are shown, n = 3. The micrographs were recorded using an inverted phase-contrast light microscope. Arrow = cell shrinkage and blebbing; dashed arrow = cytoplasmic vesicles.

XN effect on nuclear chromatin

The effect of XN on nuclear chromatin was analyzed following treatment of cells with different concentrations of XN (Figure 4). Chromatin changes were determined using nuclear staining

dye, Hoechst 33258, and then the cells were examined using fluorescent microscopy. Cells

treated with different concentration of XN displayed nuclear chromatin changes such as

chromatin condensation which fluoresced bright blue (arrow), whereas control cells stained dark

blue without bright blue staining and displayed a normal, round, and unpunctuated nucleus (Figure 4A). The cells treated with XN showed condensed and fragmented nuclei which displayed bright blue fluorescent appearance compared with control, and these cells were scored as apoptotic cells (Figure 4A, dashed arrow). XN significantly increased the number of apoptotic cells at concentration higher than 6.25 µM compared to control (Figure 4B). The number of

A

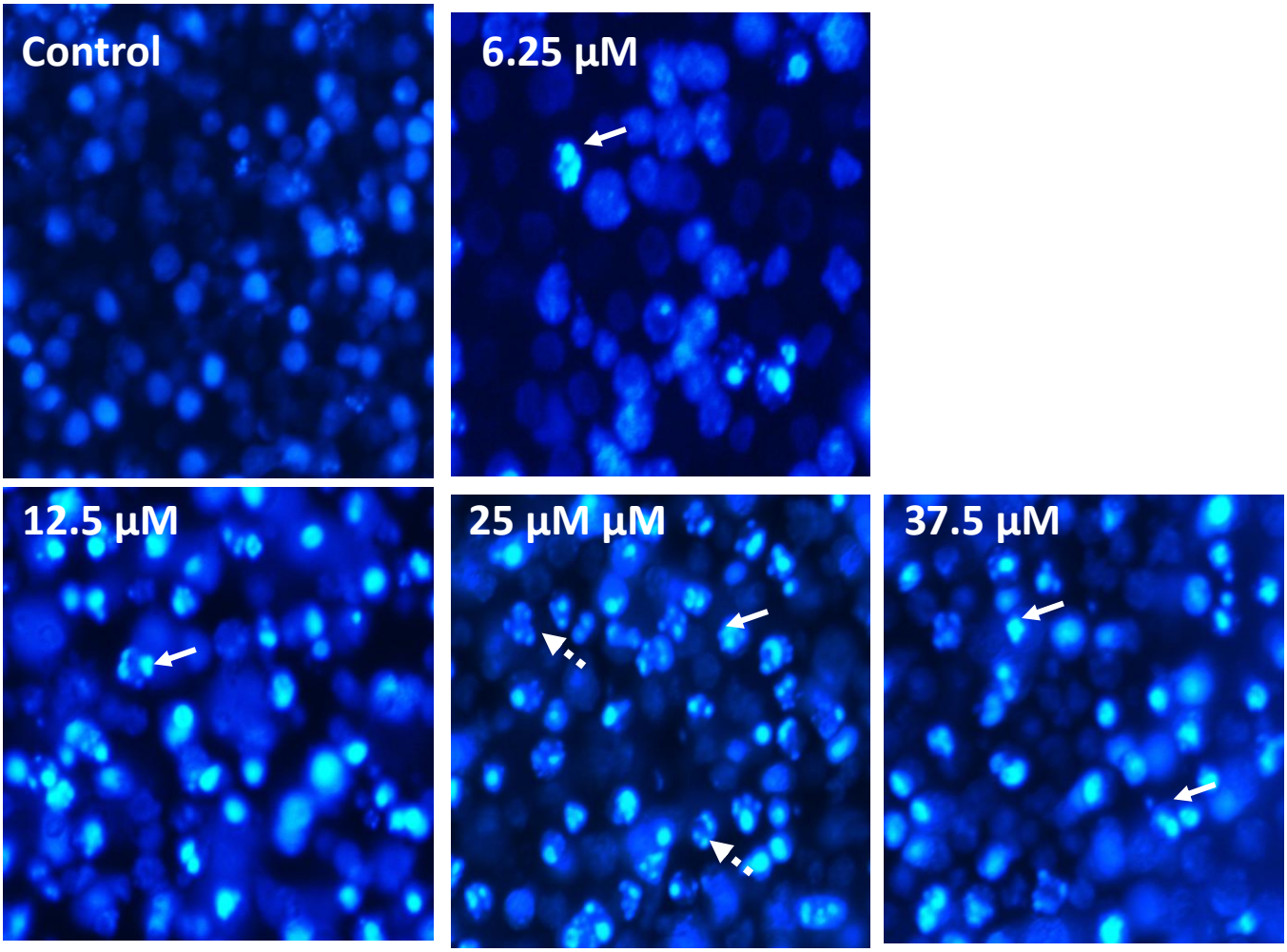

apoptotic cells was significantly higher when the cells were treated with 12.5, 25, or 37.5 µM of XN having a 21-, 40.5 and 42.2-fold increase in the number of apoptotic cells compared to control, respectively ($p < 0.05$, Figure 4B).

B

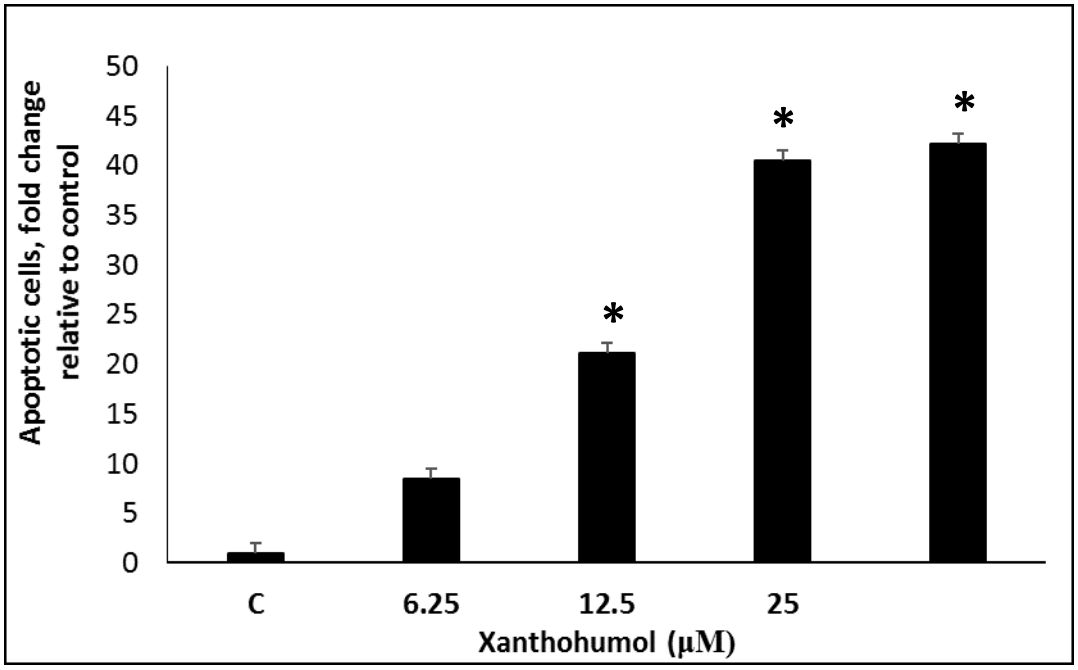

Figure 4. The effect of XN on nuclear morphology. HL-60 cells were cultured on cover slips in 5% FBS growth media for 24 h then treated with different concentrations of XN (µM) as shown in the figure for 24 h. After the treatment, the cells were stained with Hoechst 33258 and analyzed as described in Materials and Methods. A) The micrographs were taken with a fluorescent microscope. One representative micrograph is shown, n = 3. The arrow indicates condensed chromatin and condensed nuclei and were counted as apoptotic cells; punctuated nuclei = dashed arrow. B) The percentage of apoptotic cells relative to control. The values are the mean of two independent experiments, with 100 cells counted under each condition and experiment. * Statistically significant, ANOVA, $p < 0.05$ vs control.

XN induces PARP-1 cleavage

To identify which pathway of apoptosis XN activates, we analyzed PARP-1 cleavage (cPARP-

1). The cells were treated with 6.25 or 12.5 µM of XN and cell lysates was subjected to Western

blot analysis for cPARP-1 (Figure 5A). cPARP-1 level was significantly increased by both concentrations, 6.25 and 12.5 μM, of XN compared to control ($p < 0.05$, Figure 5B).

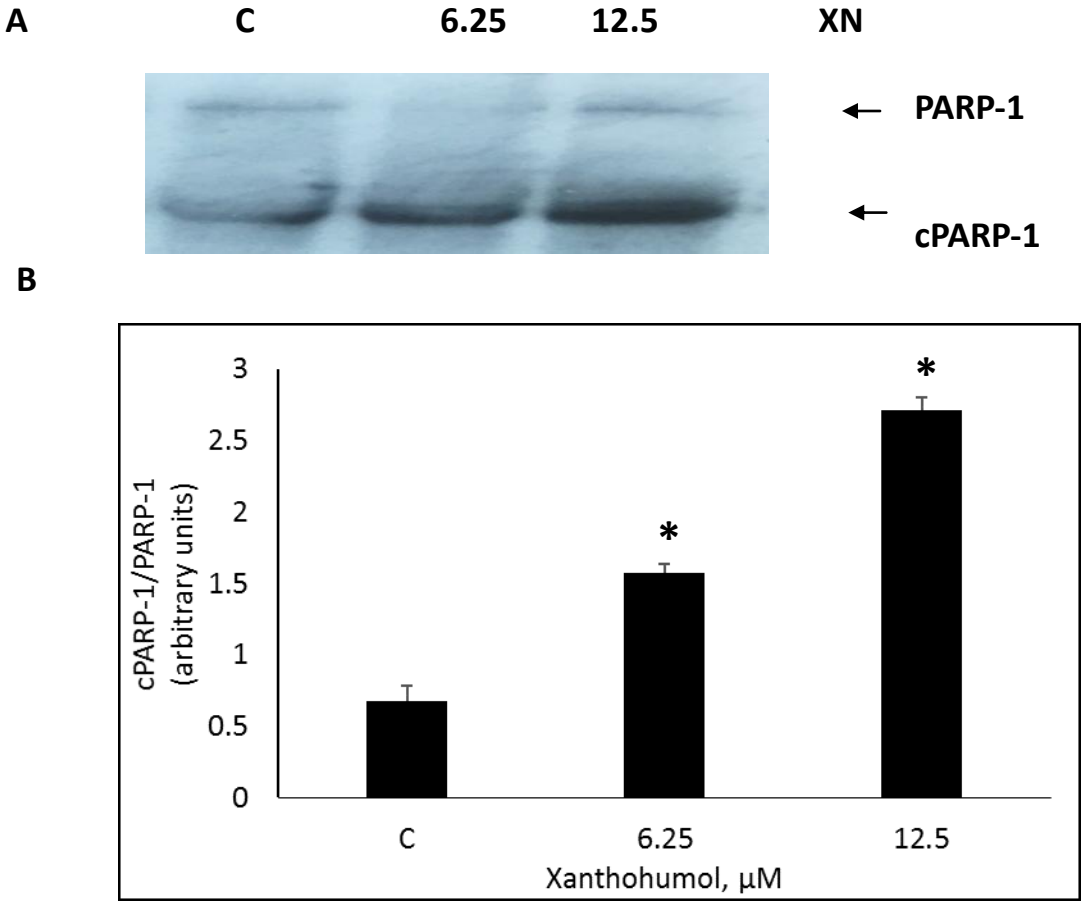

Figure 5. XN increase cPARP-1 level. HL-60 cells were cultured in 5% FBS growth media for 24 h then treated with 5 or 12.5 μM of XN for an additional 24 h. After the treatment, the cells were lysed and cell lysate was subjected to Western blot analysis as descried in Materials and Methods. One representative blot is shown. B) cPARP-1 quantitative analysis (arbitrary units), n = 3. * Statistically significant, ANOVA, $p < 0.05$ vs control.

XN activates caspase-3

To further investigate the mechanism by which XN induces HL-60 cytotoxicity, we performed additional experiments to detect active caspase-3 level. Using active caspase-3 ELISA, the analysis indicated that HL-60 cells treated with 6.25 or 12.5 μM of XN had a significant increase of active caspase-3 level (Figure 6). In samples treated with 25 μM of XN, active caspase-3 level was not significantly different compared to control samples (Figure 6).

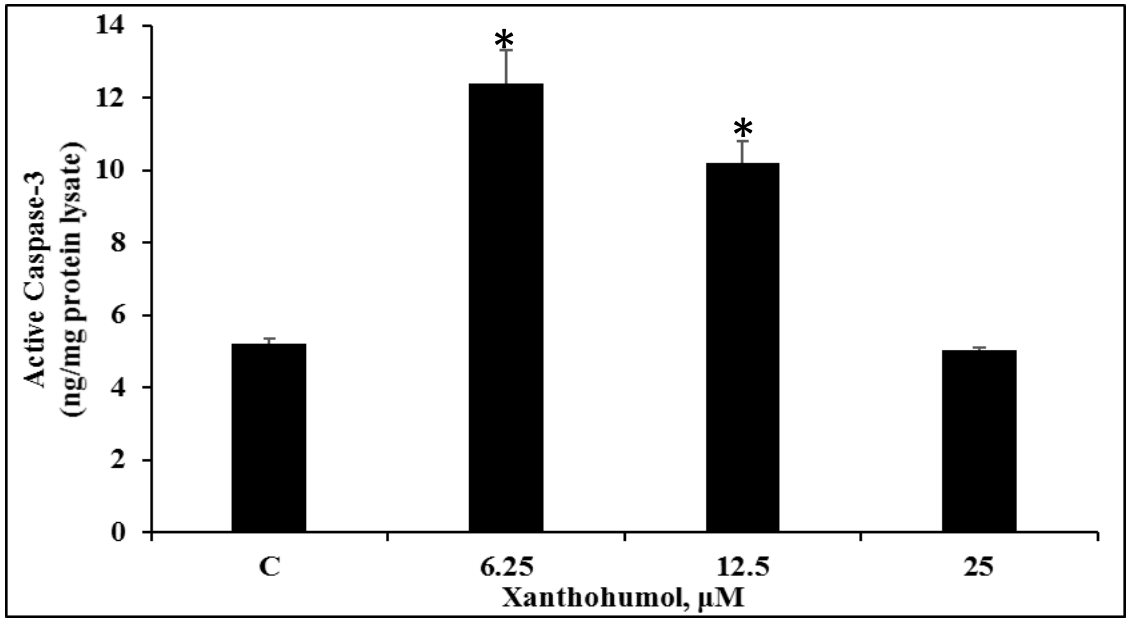

Figure 6. XN activates caspase-3. HL-60 cells were cultured in 5% FBS growth media for 24 h and then treated with 6.25, 12.5, or 25 μM of XN for an additional 24 h. After the treatment, the cells were lysed and cell lysate was subjected to caspase-3 assay as descried in Materials and Methods. The data represents mean ± SEM, n = 4. *Statistically significant, ANOVA, $p < 0.05$ vs control.

XN effects on p21$^{WAF1/Chip1}$

To further determine the mechanism by which XN inhibits cell growth, we performed an analysis on cell cycle control gene p21. Cells treated with 12.5 μM of XN had an 18.3-fold increase of p21 mRNA compared to control (Figure 7).

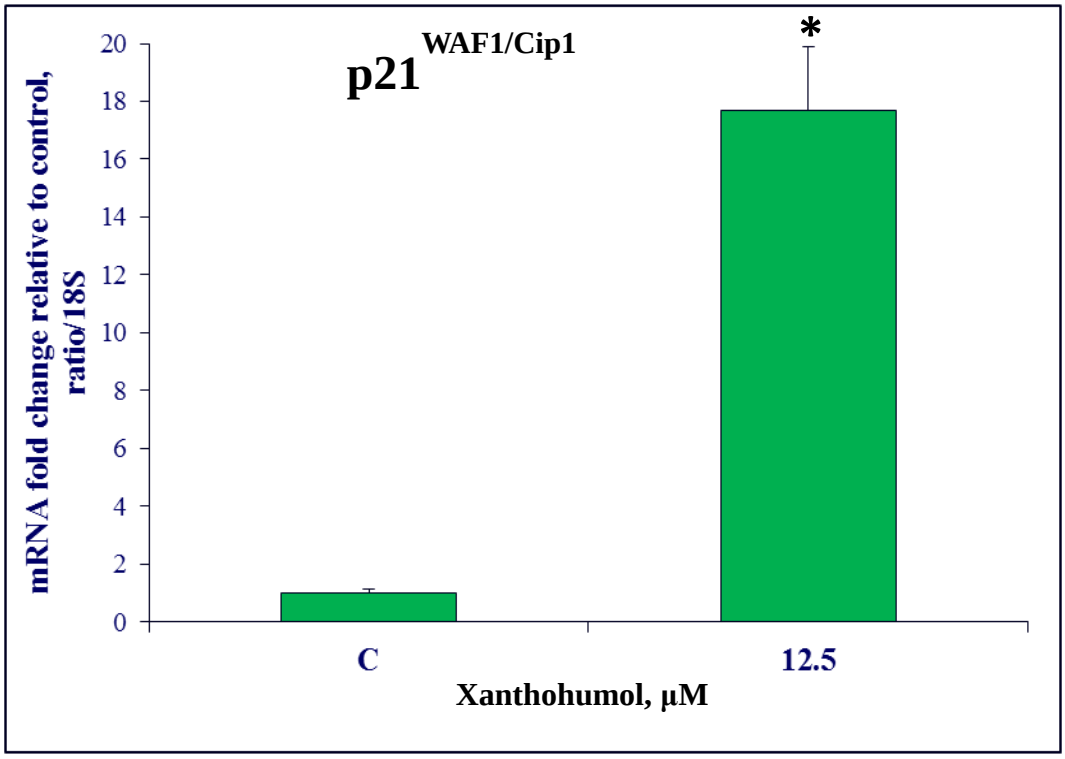

Figure 7. XN increases p21$^{WAF1/Cip1}$ mRNA. HL-60 cells were treated with 12.5 μM of XN for 24 h and RNA and qPCR were performed as described in Materials and Methods. The data is represents mRNA fold change relative to 18S. The data represents the mean ± SEM, n = 4. * Statistically significant, ANOVA, $p < 0.05$ vs control**.**

Discussion

AML relapse is often observed regardless of the initial cytotoxic effect of traditional chemodrugs [35]. The exact mechanisms of how and why AML relapses are not fully understood, however it is thought that acquisition of resistance to the initial treatment and accumulation of mutations may contribute to AML relapse [36]. To aid in alleviating less desirable chemotherapy outcome

including chemo-resistance and side-effects, plant-based natural products are becoming of interest moreover as natural-derived products have guided the development of anti-cancer agents initially. For example, the discovery of paclitaxel in the bark of Pacific yew led to anticancer drug paclitaxel that is used to treat cancer particularly breast and non-small cell lung cancer [37]. Similarly, vinblastine and vincristine are also the first plant-based alkaloids clinically used to treat various cancers including leukemia in children. However, both vinblastine and vincristine are often associated with peripheral nerves toxicity [14, 38].

Hop plant cones contain prenylated flavonoids among which XN have been shown to have cytotoxic effects and to modulate carcinogenesis [39-40]. Numerous studies analyzing biological activity showed that XN is antiproliferative and antitumor [41-43]. The mechanisms through which XN exerts its antitumor properties includes inhibition of alkaline phosphates and upregulation of cell cycle genes in the G0/G1 phase including p21 [40, 43]. In the present study, we show that XN inhibited HL-60 cells proliferation is a dose-dependent manner, and that at the highest tested dose of 50 μM, only 21% of cell were viable. To further investigate the mechanism involved in the cytotoxic effect of XN, we analyzed chromatin condensation. We used Hoechst 33258 staining to determine apoptotic cells and we found that XN dose-dependently increased the number of apoptotic cells. XN induced typical apoptotic nuclear morphology including chromatin condensation and nuclear fragmentation.

Apoptosis is a well-organized cellular process in a sequence of steps that lead to the elimination of cells under normal physiological conditions. However in tumor cells, apoptosis is an induced process primarily by chemotherapy [44]. In the present study, we examined the mechanism of apoptosis induced by XN in HL-60. XN significantly increased active capsase-3 level by 2.39- and 2-fold compared to control at 6.25 and 12.5 μM, respectively. At 25 μM,

caspase-3 was not significantly different from control. Nuclear staining showed that at the same concentration of 25 μM, 85% of cells displayed condensed and fragmented chromatin, indicating that at this concentration XN's cytotoxic effect was profound. To further determine XN apoptotic mechanism, Western blot analysis showed that XN activated PARP-1 cleavage. Cleaved PARP-1 is a hallmark of apoptosis [45]. While many caspases cleave PARP-1, caspase-3 has been shown to cleave PARP-1. Our data indicate that XN increased active caspase-3 level at 6.25 μM and increased PARP-1 cleavage at 12.5 μM, thus suggesting that capase-3 activation proceeds PARP-1 cleavage. Soldani et al. [46] monitoring PARP-1 in Hep2 cells found that PARP-1 cleavage takes place after caspases activation and the larger fragment of PARP-1, p89, is detected in the cells undergoing apoptosis and also have profound nuclear fragmentation. To further understand cytotoxic effect of XN, we investigated its effect on $p21^{WAF1/CIP1}$ mRNA. XN at 12.5 μM increased p21 mRNA by 18-folds compared to control. $p21^{WAF1/CIP1}$ is a member of the CDKIs that inhibits G1 cyclin/Cdks thus arresting cell cycle progression in the G1/S phase [47-48]. Additionally, p21 modulates cell apoptosis [48-49].

Conclusions

The present study demonstrates that XN significantly decreased HL-60 cells viability and induced apoptosis through the activation of PARP-1 cleavage and up-regulation p21 gene that controls cell cycle in the G1/S phase. These results suggest that XN induces leukemia cells death and warrants potential therapeutic investigation.

Acknowledgements

This work was supported by NIH/NIGMS Grant No. R25GM067122 through RISE at Jackson State University and Jackson State University President's Creative Award to MP. The funding sources listed had no role in study design, data collection and analysis, interpretation or writing of the manuscript.

Authors' contributions

Author Pacurari M designed the study and Brown H and Rieland A performed the experiments and statistical analysis, and wrote the first draft of the manuscript. All authors managed the analyses of the study. All authors read and approved the final manuscript.

Competing conflicts

The authors have no conflict of interest to declare.

References

1. Yamamoto JF, Goodman MT. Patterns of leukemia incidence in the United States by subtype and demographic characteristics, 1997-2002. Cancer Causes Control. 2008; 19:379-390.

2. Elbahesh E, Patel, Tabbara IA. Treatment of acute promyelocytic leukemia. Anticancer Res. 2014; 34:1507-1517.

3. Huang J, Sun M, Wang Z, Zhang Q, Lou J, Cai Y, Chen W, Du X. Induction treatments for acute promyelocytic leukemia: a network meta-analysis. Oncotarget. 2016; 7:71974–71986.

4. Dores GM, Devesa SS, Curtis RE, Linet MS, Morton LM. Acute leukemia incidence and patient survival among children and adults in the United States, 2001-2007. Blood. 2012; 119:34–43

5. Jabo B, Morgan JW, Martinez ME, Ghamsary M, Wieduwilt MJ. Sociodemographic disparities in chemotherapy and hematopoietic cell transplantation utilization among adult acute lymphoblastic and acute myeloid leukemia patients. PLoS One. 2017; 12:e0174760.

6. Kamath GR, Tremblay D, Coltoff A, Caro J, Lancman G, Bhalla S, Najfeld V, Mascarenhas J, Taioli E. Comapring the epidemiology, clinical characteristics and prognostic factor of acute myeloid leukemia with and without acute promyelocytic leukemia. Carcinogenesis. 2019; 40:651-660.

7. Breccia, M., et al. Early hemorrhagic death before starting therapy in acute promyelocytic leukemia: association with high WBC count, late diagnosis and delayed treatment initiation. Haematologica. 2010; 95:853-4.

8. Robak T, Wierzbowska A. Current and emerging therapies for acute myeloid leukemia. Clin Ther. 2009; 31:1346-2370.

9. Calgarotto AK, Maso V, J.unior GC, Nowill AE, Filho PL, Vassallo J, Saad STO. Antitumor activities of quercetin and green tea in xenografts of human leukemia HL-60 cells. Sci Rep. 2018; 8:3459.

10. Chabner BA. In: Goodman & Gilman's The Pharmacological Basis of Therapeutics. 11th Edition. Brunton LL, Lazo JS, Parker KL, editors New York. 2006; 1257–1262 (McGraw-Hill).

11. Guérritte F. On: Anticancer Agents from Natural Products. Cragg GM, Kingston DGI, Newman DJ. Editors Boca Raton, FL. 2005; 123–135 (CRC/Taylor & Francis).

12. Bellmunt J, Albanell H, Gallego OS, Ribas A, Vicente P, Carulla H, De Torres J, Morote J, Lopez M, Sole LA. Carboplatin, methotrexate, and vinblastine in patients with bladder cancer who were ineligible for cisplatin-based chemotherapy. Cancer. 1992; 70:1974-9.

13. Fraschini G, Yap HY, Hortobagyi GN, Buzdar A, Blumenschein G. Five-day continuous-infusion vinblastine in the treatment of breast cancer. Cancer. 1985; 56:225-9.

14. Vainionpaa L, Kovala T, Tolonen U, Lanning M. Vincristine therapy for children with acute lymphoblastic leukemia impairs conduction in the entire peripheral nerve. Pediatric Neurol. 1995; 13:314–8.

15. Varedi M, Ness KK, McKenna RF. Balance deficits in long-term pediatric ALL survivors. Oncotarget. 2008; 9:32554-32555.
16. Torello CO. Reactive oxygen species production triggers green tea-induced anti-leukemic effects on acute promyelocytic leukemia model. Cancer Lett. 2017; 10:116–126.
17. Hao Y, Zhang N, Wei N, Yin H, Zhang Y, Xu H, Zhou C, Doujie Li. Matrine induces apoptosis in acute myeloid leukemia cells by inhibiting the PI3K/Akt/mTOR signaling pathway. Oncol Lett. 2019; 18:2891-2896.
18. Roehrer S, Stork V, Ludwig C, Minceva M, Behr J. 2019. Analyzing bioactive effects of the minor hop component xanthohumol C on human breast cancer cells using quantitative proteomics. PLOS One. 2019; 14:e0213469.
19. Zanoli P; Zavatti M. Pharmacognostic and pharmacological profile of Humulus lupulus L. J. Ethnopharmacol. 2008; 116:383–396.
20. Vogel S, Barbic M, Jürgenliemk G, Heilmann J. Synthesis, cytotoxicity, anti-oxidative and anti-inflammatory activity of chalcones and influence of A-ring modifications on the pharmacological effect. Eur J Med Chem. 2010; 45:2206-13.
21. Aydin T, Bayrak N, Baran E, Cakir A. Insecticidal effects of extracts of *Humulus lupulus (hops) L* cones and its principal component, xanthohumol. Bull Entomol Res. 2017; 10:543-549.
22. Lupinacci E, MeiJ.erink J, Vincken JP, Gabriele B, Gruppen H, Witkamp RF. Xanthohumol from hop *(Humulus lupulus L.)* is an efficient inhibitor of monocyte chemoattractant protein-1 and tumor necrosis factor-alpha release in LPS-stimulated RAW 264.7 mouse macrophages and U937 human monocytes. J Agric Food Chem. 2009; 57:7274–81.
23. Gerhauser, C, Alt A, Heiss E, Gamal-Eldeen, Klimo K, Knauft J, Neumann I, Scherf R, Frank N, Bartsch H, Becker H. Cancer chemopreventive activity of xanthohumol, a natural product derived from hop. Mol Cancer Ther. 2001; 1:959-969.
24. Dorn C, Kraus B, Motyl M, Weiss TS, Gehrig M, Schölmerich J., Heilmann J., Hellerbrand C. Xanthohumol, a chalcone derived from hops, inhibits hepatic inflammation and fibrosis. Mol Nutr Food Res. 2010; 54:S205-S213.
25. Legette LL, Luna AY, Reed RL, Miranda CL, Bobe G, Proteau RR, et al. Xanthohumol lowers body weight and fasting plasma glucose in obese male Zucker fa/fa rats. Phytochem. 2013; 91:236–41.
26. Gerhauser C, Alt A, Heiss E, Gamal-Eldeen, Klimo K, Knauft J, Neumann I, Scherf R, Frank N, Bartsch H, Becker H. Cancer chemopreventive activity of xanthohumol, a natural product derived from hop. Mol Cancer Ther. 2002; 1:959-969.
27. Kunnimalaiyaan S, Trevino J., Tsai S, Gamblin TC, Kunnimalaiyaan M. Xanthohumol-mediated suppression of Notch1 signaling is associated with antitumor activity in human pancreatic cancer cells. Mol Cancer Ther. 2015; 14:1395-403.
28. Sun Z, Zhou C, Liu F, Zhang W, Chen J., Pan Y, Ma L, Liu Q, Yang J., Wang Q. Inhibition of breast cancer cell survival by xanthohumol via modulation of the Notch signaling pathway in vivo and in vitro. Oncol Lett. 2018; 15:908-916.
29. Venturelli S, Burkard M, Biendl M, Lauer UM, Frank J., Busch C. Prenylated chalcones and flavonoids for the prevention and treatment of cancer. Nutr. 2018; 8:S0899-9007.
30. Slawinska-Brych A, Zdzisinska B, Dmoszynska-Graniczka M, Jeleniewicz W, Kurzepa J, Gagos M, Stepulak A. Xanthohumol inhibits the extracellular signal regulated (ERK) signaling pathway and suppresses cell growth of lung adenocarcinoma cells. Toxicol. 2016; 357:65-73.
31. Yong WK, Abd Malek SN. Xanthohumol induces growth inhibition and apoptosis in Ca Ski human cervical cancer cells. Evid Based Complement Alternat Med. 2015; 2015:921306.
32. Liu W, Li W, Liu H, Yu X. Xanthohumol inhibits colorectal cancer cells via downregulation of hexokinases II-mediated glycolysis. Int J Biol Sci. 2019; 15:2497-2508.
33. Pacurari M, Qian Y, Porter DW, Wolfarth M, Wan Y, Luo D, Ding M, Castranova V, Guo N L. Multi-walled carbon nanotube-induced gene expression in the mouse lung: Association with lung pathology. Toxicol Appl Pharmacol. 2011; 255:18–31.

34. Pacurari M, Addison BJ, Bondalapati N, Wan YW, Luo D, Qian Y, Castranova V, Ivanov AV, Guo N. The microRNA-200 family targets multiple non-small cell lung cancer prognostic markers in H1299 cells and BEAS-2B cells. Intern J Oncology. 2013; 43:548-560.
35. Ramos NR, Co CC, Karp JE, Hourigan CS. Current approaches in the treatment of relapsed and refractory acute myeloid leukemia. J Clin Med. 2015; 4:665-695.
36. Corces-Zimmerman MR, Hong WJ, Weissman IL, Medeiros BC, MaJeti R. Preleukemic mutations in human acute myeloid leukemia affect epigenetic regulators and persist in remission. Proc Natl Acad Sci, USA. 2014; 111:2548-2553.
37. Unnati S, Ripal S, SanJ.eev A, Nuyati A. Novel anticancer agents from plants. Chinese J of Nat Med. 2013; 11:0016-0023.
38. Kumar A. Vincristine and vinblastine: a review. Intel J Med Pharm Sci. 2016; 6:23-30.
39. Arimoto-Kobayashi S, Sugiyama C, Harada N, Takeuchi M, Takemura M, Hayatsu HJ. Inhibitory effects of beer and other alcoholic beverages on mutagenesis and DNA adduct formation induced by several carcinogens. Agric Food Chem. 1999; 47:221–230.
40. Miranda CL, Stevens JF, Helmrich A, Henderson MC, Rodriguez RJ, Yang YH, Deinzer ML, Barnes DW, Buhler DR. Antiproliferative and cytotoxic effects of prenylated flavonoids from hop (Humulus lupulus) in human cancer cell lines. Food Chem Toxicol. 1999; 37:271 –285.
41. Gerhauser C, Alt A, Heiss E, Gamal-Eldeen, Klimo K, Knauft J, Neumann I, Scherf R, Frank N, Bartsch H, Becker H. Cancer chemopreventive activity of xanthohumol, a natural product derived from hop. Mol Cancer Ther 2002; 1:959-969.
42. Li Y, Wang K, Yin S, Zheng H, Min D. Xanthohumol inhibits proliferation of laryngeal squamous cell carcinoma. Oncol Lett. 2016; 12:5289-5294.
43. Sun Z, Zhou C, Liu F, Zhang W, Chen J., Pan Y, Ma L, Liu Q, Yang J., Wang Q. 2018. Inhibition of breast cancer cell survival by xanthohumol via modulation of the Notch signaling pathway in vivo and in vitro. Oncol Lett. 2018; 15:908-916.
44. Cao B, Chen H, Gao Y, Niu C, Zhang Y, Li L. CIP-36, a novel topoisomerase II-targeting agent, induces the apoptosis of multidrug-resistant cancer cells in vitro. Int J Mol Med. 2015; 35:771–776.
45. Kaufmann SH, Desnoyers S, Ottaviano Y, Davidson NE, Poirier GG. Specific proteolytic cleavage of poly(ADP-ribose) polymerase: an early marker of chemotherapy-induced apoptosis. Cancer Res. 1993; 53:3976–3985.
46. Soldani C, Lazze MC, Bottone MG, Tgnon G, Biffigera M, Pellieciari CE, Scoassi AI. Poly(ADP-ribose) polymerase cleavage during apoptosis: When and Where. Exp Cell Res. 2001; 269:193-201.
47. Harper JW, Adami GR, Wei N, Keyomarsi K, Elledge SJ. The p21 Cdk-interacting protein Cip1 is a potent inhibitor of G1 cyclin-dependent kinases. Cell. 1993; 75:805-16.
48. Sherr CJ, Roberts JM. CDK inhibitors: positive and negative regulators of G1-phase progression. Genes Dev. 1999; 13:1501–12.
49. Coqueret O. 2003. New roles for p21 and p27 cell-cycle inhibitors: a function for each cell compartment? Trends Cell Biol. 2003; 13:65-70.